Forced convective heat transfer from premixed flames

—Part 2: Impingement heat transfer

G. K. Hargrave*†, M. Fairweather*† and J. K. Kilham*

A study of convective heat transfer from impinging flames is completed with the presentation of heat transfer rates measured in premixed methane–air flames. Unburnt gas equivalence ratios from 0.8 to 1.2 have been examined, with burner exit Reynolds numbers ranging from 2000 to 12 000. Heat fluxes measured at the stagnation point of a body of revolution and a circular cylinder demonstrate that the trends observed in measured heat flux profiles are mainly determined by variations in the mean velocity and temperature within a flame, with peak heat transfer rates occurring within or close to the flame reaction zone. Increases in Reynolds number lead to an increase in the peak heat flux attained within a flame and to a decrease in the axial extent of the flame equilibrium region. Variations in equivalence ratio away from approximately stoichiometric conditions lead to a decrease in the maximum rate of heat transfer from a flame and to a shifting of the position of maximum flux downstream. Theoretical predictions applicable to the equilibrium region of the flames are in reasonable accord with experimental data.

Keywords: *heat transfer, convection, flames, methane, impingement, stagnation point*

Introduction

The work described in this paper is the second part of a study of convective heat transfer from impinging flames. The overall objective of the study has been to gain an understanding of the relationship between the local properties of premixed flames and the heat transfer that results when such flames impinge upon a body.

In the first part of the study[1] the aerodynamic structure of four flames was examined. These flames were of stoichiometric mixtures of methane and air with a burner exit Reynolds number range of 2000 to 12 000. This Reynolds number range ensured the study of both laminar and fully developed turbulent flames. Measurements of mean and rms velocities and mean temperatures were made within the flames, and instantaneous Schlieren photography and Schlieren-stroboscopic techniques were used to examine the visual appearance of the flames. Results obtained for the effect of Reynolds number on flame structure, reported in Ref 1, are also qualitatively representative of nonstoichiometric flames.

The heat transfer that results when premixed methane–air flames impinge upon bodies is the subject of the present paper. In addition to the flames examined in the first part of the study, impingement heat transfer from flames with equivalence ratios from 0.8 to 1.2 over the 2000 to 12 000 Reynolds number range has also been considered. Heat transfer measurements have been made at the stagnation point of a body of revolution (hemispherical-nosed cylinder) and a circular cylinder. The stagnation point of a convex surface placed in a high temperature free stream flow represents the position of maximum heat flux, and heat transfer measurements made in the vicinity of this point are therefore important for design purposes and for assessing maximum material stress.

* Department of Fuel and Energy, The University, Leeds LS2 9JT, UK
† Present address: British Gas Corporation, Midlands Research Station, Solihull B91 2JW, UK
Address for correspondence: Dr. M. Fairweather, British Gas Corporation, Midlands Research Station, Wharf Lane, Solihull, West Midlands B91 2JW, UK
Received 9 April 1986 and accepted for publication on 8 September 1986

0142-727X/87/020132-07$3.00

Experimental work

Measurements of heat flux at the stagnation point of a hemispherical-nosed cylinder and a circular cylinder were made using the two calorimeters illustrated in Fig 1.

A steady-state calorimeter (Fig 1(a)) was constructed for the measurement of heat flux at the stagnation point of a 22 mm diameter hemispherical-nosed body. This calorimeter was a conductivity type heat flow meter consisting of a uniform rod along which heat is conducted. In the present device one end of a 3.2 mm diameter and 110 mm long copper rod was exposed to flame gases at the stagnation point of the probe, whilst the other end of the rod was soldered into a brass block which was maintained at a constant temperature using a controlled water flow. Four insulated 0.25 mm constantan wires were soldered into 0.8 mm holes in the copper rod to form thermocouples at the positions indicated in Fig 1(a). These thermocouples allowed the heat flux incident on the end of the rod exposed to the flame gases to be calculated from measured temperature differences and the known thermal properties of copper.

Surrounding the rod was a copper tube which acted as a radiation shield. This tube was machined so that over most of its length it had the same cross-sectional area as the copper rod. The shield was exposed to flame gases at one end and cooled with water flow at the other so that it possessed the same temperature gradients as the rod. The shield therefore prevented the rod from losing heat by radiation and, because the shield and rod were separated by a narrow air gap, it also stopped heat loss by convection. The body and hemispherical nose of the probe were formed by a hollow brass sheath. This sheath was cooled using ethylene glycol which was maintained at a temperature of 378 K in order to prevent the condensation of water vapour in the flame gases on the surface of the probe. The calorimeter was calibrated experimentally using a black body furnace in order to avoid inaccuracies that occur in theoretical calibrations on account of unpredictable heat losses. Measurements of heat flux obtained using the steady-state probe were for an average temperature of the exposed calorimeter surface of 418 K.

A transient calorimeter (Fig 1(b)) was constructed for the measurement of heat flux at the stagnation point of a 22 mm diameter cylindrical body. The calorimeter used was a slug type

calorimeter consisting of an insulated cylinder, or slug, of metal with a thermocouple attached to its back face. When the front face of the slug is then exposed to a uniform heat flux the rate of temperature rise on the back face is directly proportional to the incident flux. In the present device a 3.2 mm diameter by 1.0 mm thick copper slug was fixed at the stagnation point of a 250 mm long solid brass cylinder using low conductivity epoxy resin. A chromel–alumel thermocouple was used to monitor the temperature of the rear surface of the slug.

Unlike the steady-state calorimeter, which could be exposed to flame gases for relatively long periods of time, operation of the transient device consisted of rapidly exposing the probe to the flame gases using a pair of push–pull solenoids. Instantaneous temperatures at the rear surface of the slug were monitored using a microcomputer-based data logging system, and the rate of temperature rise over a chosen temperature interval was then used to calculate the heat flux incident on the exposed surface[2,3]. Measured heat fluxes were corrected for heat losses by calibrating the transient device, mounted in a hemispherical-nosed body, against the steady-state heat flux probe described above. Measurements of heat flux obtained using the transient probe were for an average temperature of the exposed calorimeter surface of 378 K.

Despite the apparent size of the two probes, Schlieren techniques showed that the presence of either of the probes in a flame had little effect on the visible appearance of the flames examined or on the low frequency flame oscillations reported in the first part of the study. The results given later to some extent confirm that the structure of the flames was not significantly affected by the probes. Also, because the transient probe was exposed to the flames for relatively short periods of time, it was important to ensure that the exposure time was sufficiently long for measured heat fluxes to be unaffected by flame oscillations. The suitability of the time period employed was checked for the worst case of the $Re = 2000$ flames, where the lowest frequency oscillations in mean velocity were observed, by repeating the heat flux measurements in these flames. In those parts of these flames affected by oscillations the scatter in the results obtained was on average 3%.

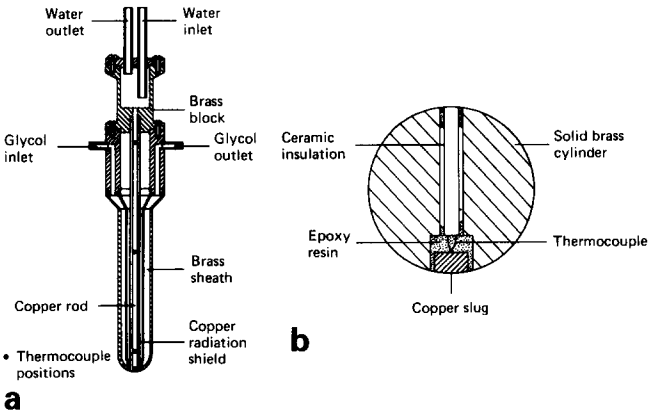

Figure 1 Schematic of (a) the steady-state calorimeter (body of revolution) and (b) the transient calorimeter (cylinder)

Theoretical work

Measured free stream properties were used to enable theoretical predictions of impingement heat transfer from numerical solutions of the boundary layer equations, and from empirical correlations derived for nonreacting flows.

The turbulent boundary layer equations applicable to compressible, multicomponent reacting flows may be written as[4]

$$\frac{\partial}{\partial x}(\rho u r^n) + \frac{\partial}{\partial y}(\rho v r^n) = 0 \tag{1}$$

$$\rho u \frac{\partial u}{\partial x} + \rho v \frac{\partial u}{\partial y} = -\frac{dp_e}{dx} + \frac{\partial}{\partial y}\left[(\mu + \varepsilon)\frac{\partial u}{\partial y}\right] \tag{2}$$

$$\rho u \frac{\partial h}{\partial x} + \rho v \frac{\partial h}{\partial y} = \frac{\partial}{\partial y}\left[\left(\frac{\mu}{Pr_{eq}} + \varepsilon\right)\frac{\partial h}{\partial y}\right] + \frac{\partial}{\partial y}\left[\frac{\mu}{2}\left(1 - \frac{1}{Pr_{eq}}\right)\frac{\partial u^2}{\partial y}\right] \tag{3}$$

where $n = 0$ for a two-dimensional body and $n = 1$ for a body of revolution, and all dependent variables are time-averaged values. In writing these equations chemical equilibrium of the flow field has been assumed, and the reacting thermal conductivity concept of Butler and Brokaw[5] employed in order to simpify the analysis. Closure is by Boussinesq's eddy diffusivity concept, and turbulent Lewis and Prandtl numbers of one have been assumed.

Using a stream function defined to satisfy the continuity equation in the normal way, the partial differential equations for

Notation

C	Ratio of $\rho\mu$ at a point in boundary layer to value at boundary layer outer edge
C_1, C_2	Constants defined in Eq (13)
C_3, C_4, C_5	Constants defined in Eq (14)
d	Diameter of heat-receiving body
f	Reduced stream function
f'	Ratio of u at a point in boundary layer to value at boundary layer outer edge
g	Ratio of h at a point in boundary layer to value of boundary layer outer edge
h	Total enthalpy
k	Thermal conductivity
K	Constant defined in Eq (9)
Nu	Nusselt number
p	Pressure
Pr	Prandtl number
q	Heat flux
r	Radius of heat-receiving body in a meridian plane
Re	Reynolds number
T	Temperature
Tu	Turbulence intensity
u	Velocity component in x direction
v	Velocity component in y direction
x	Distance along surface of heat-receiving body from stagnation point
$\bar{x}$	Transformed x coordinate
X	Downstream distance along flame centreline measured from burner port
y	Distance perpendicular to surface of heat-receiving body through boundary layer
β	Stagnation point velocity gradient
ε	Eddy viscosity
η	Transformed y coordinate
μ	Dynamic viscosity
ρ	Density
ϕ	Equivalence ratio
Subscripts	
e	Evaluated at outer edge of boundary layer
eq	Equilibrium value
w	Evaluated at body surface
∞	Free stream value
Superscripts	
$'$	Differentiation with respect to η

conservation of momentum and energy can be transformed from the (x, y) coordinate system to an alternative $(\bar{x}, \eta)$ system using the Lees–Dorodnitsyn transformations[6]. For the stagnation region the following $\bar{x}$-independent ordinary differential equations result:

$$\left[\left(1+\frac{\varepsilon}{\mu}\right)Cf''\right]'+ff''+\frac{1}{2^n}\left[\frac{\rho_e}{\rho}-(f')^2\right]=0 \tag{4}$$

$$\left[\left(\frac{1}{Pr_{eq}}+\frac{\varepsilon}{\mu}\right)Cg'\right]'+fg'=0, \tag{5}$$

with

$$\frac{df}{d\eta}=f'=u/u_e \tag{6}$$

$$g=h/h_e \tag{7}$$

$$C=\rho\mu/\rho_e\mu_e, \tag{8}$$

and where prime denotes differentiation with respect to η.

The equations derived above permit the prediction of heat transfer rates through the laminar boundary layer formed in the stagnation region of a body placed in a turbulent free stream flow. Through the eddy viscosity term they also allow for increases in heat transfer caused by the random penetration of turbulent free stream eddies into the laminar boundary layer. After Smith and Kuethe[7], and Galloway[8], homogeneous and isotropic free stream turbulence is assumed and Prandtl's mixing length concept used in order to derive an eddy law. The turbulence intensity of the free stream defined at a reference position in the flow field corresponding to the body stagnation point with the body removed is taken to be the external driving force which sets the level of velocity fluctuations in the boundary layer near the stagnation point. Thus, as the fluctuating components penetrate into the laminar boundary layer from the free stream, the fluctuating velocity is expected to be proportional to the external free stream turbulence and flow conditions. The resulting eddy law may be written as

$$\varepsilon=K\rho Tu_\infty u_\infty y \tag{9}$$

where K is a constant. For the case of turbulent nonreacting flows impinging on a body of revolution and a cylinder, this constant has been evaluated[9,10] as 0.20 and 0.37, respectively.

Eqs (4) and (5) were rewritten as a set of first-order equations and solved using Merson's method, in conjunction with a Newton iteration, in a shooting and matching technique[11] together with the boundary conditions

$$f(0)=f'(0)=\varepsilon(0)=y(0)=0,\ g(0)=g_w \quad \text{at } \eta=0 \tag{10}$$

$$f'(\infty)=g(\infty)=1 \qquad \text{as } \eta\to\infty \tag{11}$$

The heat flux received at the stagnation point was then obtained from

$$q_w=\left(\frac{\rho\mu}{Pr_{eq}}\right)_w h_e g'(0)\left(\frac{2^n\beta}{\rho_e\mu_e}\right)^{1/2} \tag{12}$$

Values of the stagnation point velocity gradient β were specified using equations of the form[9,10]

$$\beta=(C_1+C_2Tu_\infty)u_\infty/d \tag{13}$$

for constants C_1 and C_2. From previous work on nonreacting flows, C_1 and C_2 were taken as 2.67 and 9.62, respectively, for the case of a body of revolution[9], and as 3.85 and 4.90, respectively, for the case of a circular cylinder[10].

In order to provide a more tractable means of predicting heat fluxes, empirical correlations derived for impingement heat transfer from turbulent air flows were examined. Such equations typically have the form

$$NuRe^{-0.5}=C_3+C_4\left(\frac{TuRe^{0.5}}{100}\right)+C_5\left(\frac{TuRe^{0.5}}{100}\right)^2 \tag{14}$$

for constants C_3 to C_5. Rearranging Eq (14) gives

$$q_w=\left[C_3+C_4\left(\frac{TuRe^{0.5}}{100}\right)+C_5\left(\frac{TuRe^{0.5}}{100}\right)^2\right]\times\frac{Re^{0.5}k(T_e-T_w)}{d} \tag{15}$$

for

$$Re=\rho u_\infty d/\mu \tag{16}$$

and with turbulence intensity set equal to the free stream value Tu_∞. In order to allow for the large and nonlinear variation in fluid thermophysical properties which occur across a boundary layer subjected to a high temperature free stream, the thermophysical properties appearing in Eqs (15) and (16) were evaluated as weighted mean values[12]. For the stagnation region, the constants C_3 to C_5 were taken as 0.993, 5.465 and −2.375, respectively, for the case of a body of revolution[9], and as 1.071, 4.669 and −7.388, respectively, for the case of a circular cylinder[10].

The thermophysical properties of burnt gas mixtures required in the two prediction methods outlined above were determined as described in Ref 12. In calculating these properties, and in deriving the boundary layer equations given above, it was assumed that chemical reactions in the free stream and boundary layer flows are sufficiently fast to maintain local chemical equilibrium. This assumption restricts the validity of the prediction methods to distances downstream of a flame reaction zone where large nonequilibrium concentrations of labile species do not exist.

Results and discussion

Heat transfer to the body of revolution

Measurements of heat transfer to the stagnation point of the hemispherical-nosed body were made along the centreline of the $Re=2000$, 4000, 8000 and 12 000 flames. Methane–air equivalence ratios of 0.80, 0.90, 0.95, 1.00, 1.05, 1.10 and 1.20 were examined.

Fig 2 shows results obtained for the effect of Reynolds number on heat transfer for the four stoichiometric flames examined in detail in the first part of the study. This figure also indicates the approximate time-averaged extent of the reaction zone along the burner axis for each of the four flames. For the $Re=2000$ flow, the flame reaction zone is located between 38 and 39 mm from the burner port. Heat fluxes measured close to this zone are high since the mean velocity and temperature of the flame exhibit maxima in the vicinity of this zone[1], and also because of the nonequilibrium nature of the flow in this region. Thus, close to the high temperature reaction zone, large concentrations of reactive species such as atoms and free radicals exist which are able to augment convective heat transfer rates by diffusion and exothermic recombination in the boundary layer surrounding the heat-receiving body. Downstream of the reaction zone, heat fluxes decrease with the mean velocity and temperature of the flow until at approximately 60 mm the heat flux profile levels off. From this point the flame gases may be assumed to be approximately in chemical equilibrium[12], and increases in mean velocity due to buoyancy effects offset decreasing temperatures such that heat flux remains approximately constant with increasing axial distance. At 80 mm downstream, heat fluxes begin to increase as buoyancy effects become dominant, until at 100 mm the entrainment of ambient air results in a rapid decrease in temperature and hence heat transfer rates.

For the fully turbulent $Re=4000$ flow, random motions in the unburnt gas cause the reaction zone to become thicker and more diffuse. Associated with this is an averaging of reactive species concentrations over greater distances than occur in the $Re=2000$ flame, so that local concentrations of such species are decreased. Up to the flame reaction zone, heat fluxes increase

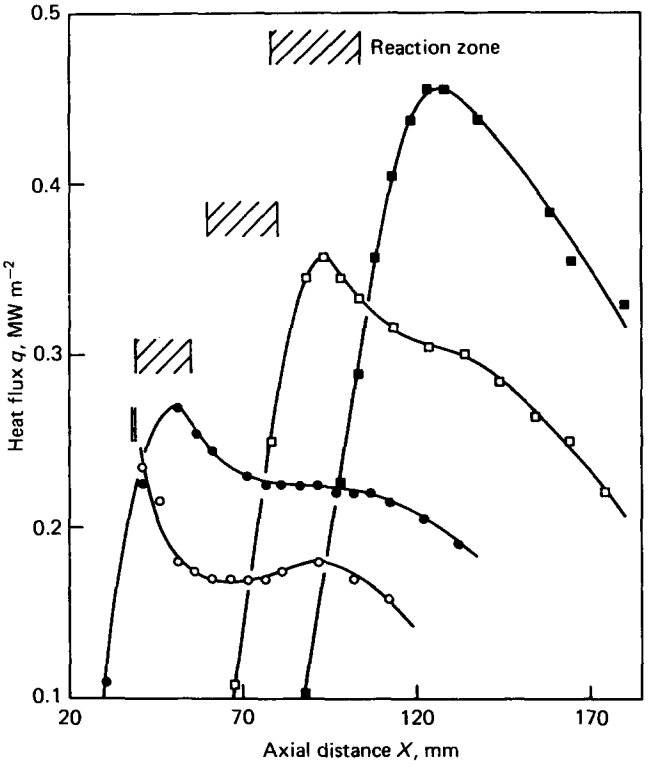

Figure 2 Effect of Reynolds number on heat transfer to the body of revolution for stoichiometric flames (○ Re=2000, ● Re=4000, □ Re=8000, ■ Re=12 000)

rapidly with mean velocity and temperature, and reach a peak towards the end of this zone which is associated with maxima in the mean velocity and temperature profiles. Downstream of the reaction zone, heat fluxes decrease with falling velocities and temperatures, with an equilibrium region being reached at approximately 80 mm. From 80 to 105 mm the heat flux remains approximately constant because velocity increases due to buoyancy again offset falling temperatures. Entrainment of cold ambient air leads to a rapid decrease in heat fluxes beyond 105 mm. Compared to the Re=2000 flame, the effect of flow turbulence in decreasing local concentrations of reactive species in the vicinity of the reaction zone leads to relatively lower heat fluxes in this region since the augmentation of heat flux by such species is decreased. This is illustrated by comparing the difference between heat fluxes obtained in the reaction zone and in the equilibrium region of the Re=4000 flame with that observed in the Re=2000 flame.

The trends exhibited by heat fluxes measured in the Re=8000 and 12 000 flames are similar to those observed for the Re=4000 case, although the higher Reynolds number flows show maxima in heat flux just downstream of the flame reaction zone. These peaks coincide approximately with maxima in the mean velocity and temperature profiles of the flames[1], although the heat flux probe may have had some slight effect on the aerodynamic structure of these two flames. Ambient air reaches the centreline of the Re=8000 and 12 000 flames at 135 and 145 mm, respectively. Compared with the Re=4000 flame, this leads to a decrease in distance between the position of maximum temperature and the point where ambient air first reaches the flame centreline in the Re=8000 flame. This in turn causes a reduction in the extent of the equilibrium region in the latter flame such that it appears essentially as an inflection in the heat flux profile. In the Re=12 000 flame, air entrainment occurs sufficiently close to the position of maximum temperature for no equilibrium region to be apparent.

The effect of Reynolds number on heat fluxes measured in nonstoichiometric flames is shown in Fig 3 for flames at the limits of the equivalence ratio range examined. Heat flux profiles in both the ϕ=0.8 (Fig 3(a)) and 1.2 (Fig 3(b)) flames are qualitatively similar to those observed in the stoichiometric flames, with increasing Reynolds number again leading to higher heat transfer rates and a reduction in the extent of the equilibrium region within the flames. Measurements of mean and fluctuating velocities and mean temperatures within these nonstoichiometric flames confirmed that the observed trends in heat flux occur for the reasons advanced above.

The variation of heat flux through the Re=2000 and 12 000 flames over the whole of the equivalence ratio range considered is shown in Figs 4 and 5, respectively. The regions of peak heat flux in these figures may be taken as an approximate indication of the position of the reaction zone within each flame. Variations of the equivalence ratio of the unburnt gas from approximately

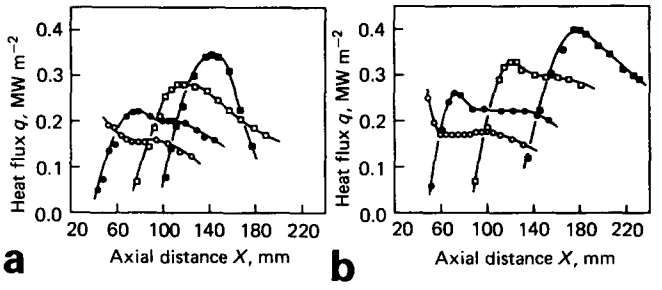

Figure 3 Effect of Reynolds number on heat transfer to the body of revolution for (a) ϕ=0.8 and (b) ϕ=1.2 flames. Key as Fig 2

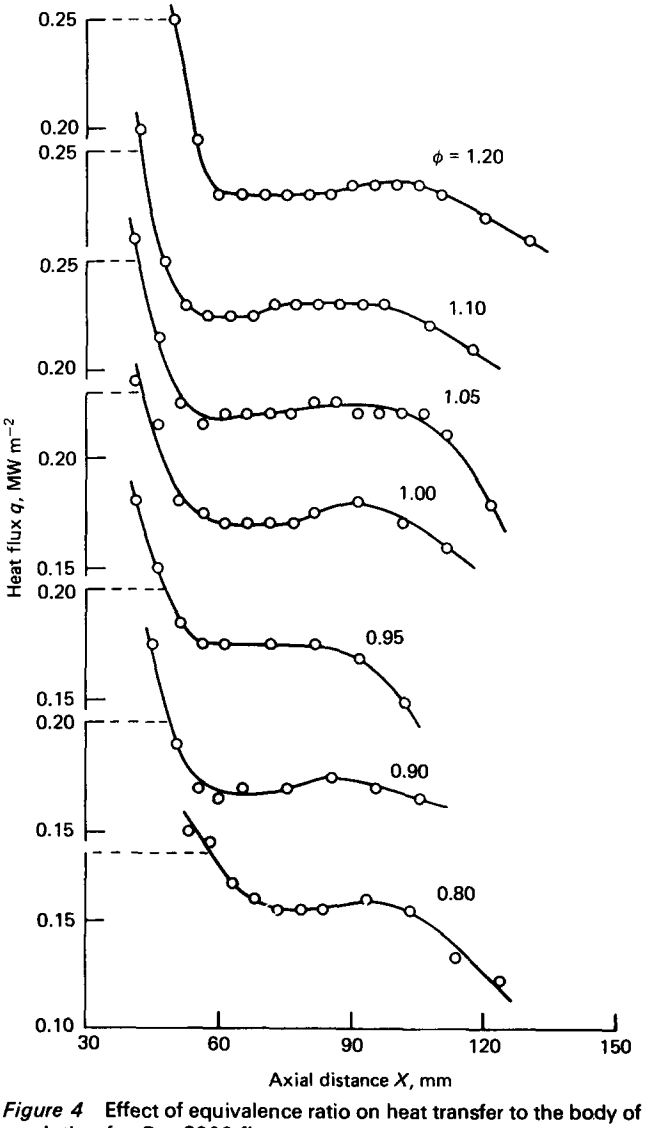

Figure 4 Effect of equivalence ratio on heat transfer to the body of revolution for Re=2000 flames

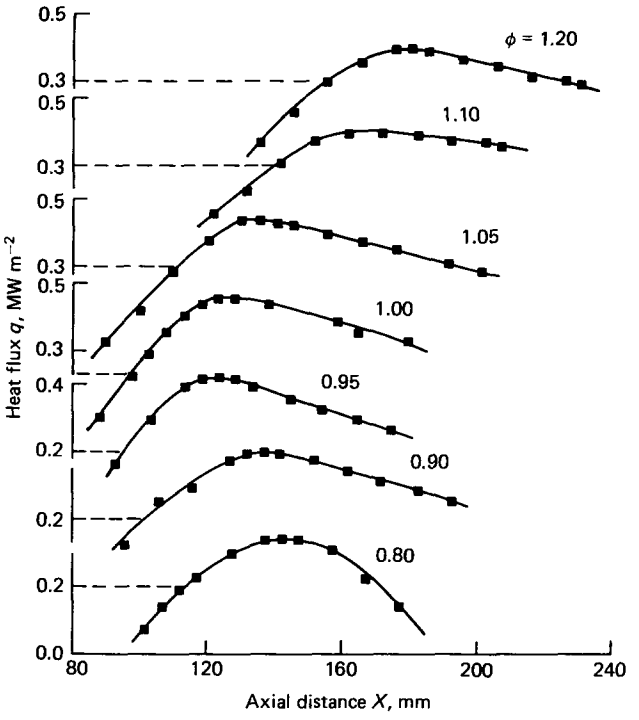

Figure 5 Effect of equivalence ratio on heat transfer to the body of revolution for $Re=12\,000$ flames

stoichiometric conditions are then seen to lead to a shifting of the reaction zone downstream for both the fuel-lean and fuel-rich flames. This movement of the reaction zone corresponds to decreases in the burning velocity of the unburnt mixture, and leads to a lengthening of the fuel-lean and fuel-rich flames. In both the $Re=2000$ and 12 000 flames the heat flux profiles exhibit the same trends over all equivalence ratios. In the $Re=2000$ flames, therefore, the extent of the equilibrium region within the flames remains approximately constant over all equivalence ratios, whilst no such region is observed in any of the $Re=12\,000$ flames. Measurements in the $Re=4000$ and 8000 flames also showed that the augmentation of heat flux due to labile species in the vicinity of the flame reaction zone, when compared with heat transfer rates measured in the equilibrium region of the flames, was a maximum for near-stoichiometric mixtures.

Fig 6 shows the variation of the maximum rate of heat transfer to the stagnation point of the hemispherical-nosed body with equivalence ratio. Data for the $Re=2000$ flames are not included in this figure because of the difficulty in measuring a peak heat flux within the thin reaction zone of these flames. In all the flames examined, peak heat fluxes occur for equivalence ratios between 1.0 and 1.1 because the highest free stream mean velocities and temperatures were observed for such mixtures.

Heat transfer to the circular cylinder

Measurements of heat transfer to the stagnation point of the circular cylinder were made along the centreline of the $Re=2000$, 4000 and 8000 flames. Methane–air equivalence ratios of 0.8, 1.0 and 1.2 were examined.

The effect of Reynolds number on heat fluxes measured in the flames is shown in Fig 7 for the stoichiometric case, and in Fig 8 for equivalence ratios of 0.8 and 1.2. The heat flux profiles shown in these figures are qualitatively similar to those obtained using the hemispherical-nosed probe, with peaks in heat flux and the position of flame equilibrium regions occurring at approximately the same axial locations. This result supports the contention that the structure of the flames was not significantly affected by the presence of the heat flux probes. A limited number of measurements made in flames with Reynolds numbers greater than 8000 also confirmed that equilibrium regions do not occur in such flames.

Comparing the data of Figs 7 and 8 with those of Figs 2 and 3 shows that, for the flames examined, heat transfer rates to the circular cylinder were greater than those obtained using the hemispherical-nosed probe at all positions in the flames. This is seen more clearly by comparing results for the variation of the maximum rate of heat transfer to the stagnation point of the cylinder with equivalence ratio, shown in Fig 9, with equivalent data for the hemispherical-nosed probe, given in Fig 6. Some of the variation between data obtained using the two probes results from differences in the temperature of the exposed calorimeter surfaces referred to previously. However, for the results shown in Figs 6 and 9, the temperature difference across the boundary layers surrounding the two bodies differed by a maximum of 5% due to variations in surface temperatures, whereas heat flux results for the cylindrical body are greater than equivalent data for the hemispherical-nosed probe by 12 to 26%. This finding is in agreement with results obtained in turbulent nonreacting jets[9,10] where, for the range of free stream Reynolds numbers and turbulence intensities encountered in the present flames, heat transfer to the stagnation point of circular cylinders was found to be greater than for hemispherical-nosed bodies.

Heat transfer predictions

Because of the assumption of chemical equilibrium used in deriving theoretical predictions the validity of results is restricted to regions in the flames away from the reaction zone. This may be illustrated by reference to Fig 10, which shows

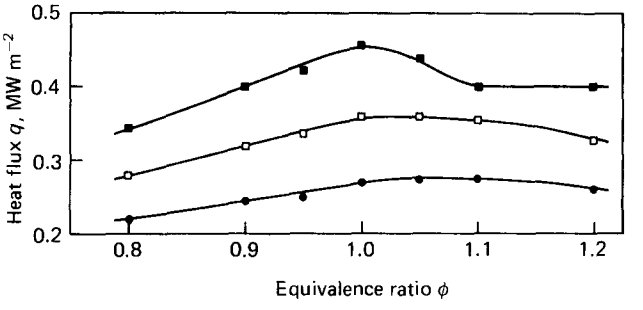

Figure 6 Variation of maximum rate of heat transfer to the body of revolution with equivalence ratio. Key as Fig 2

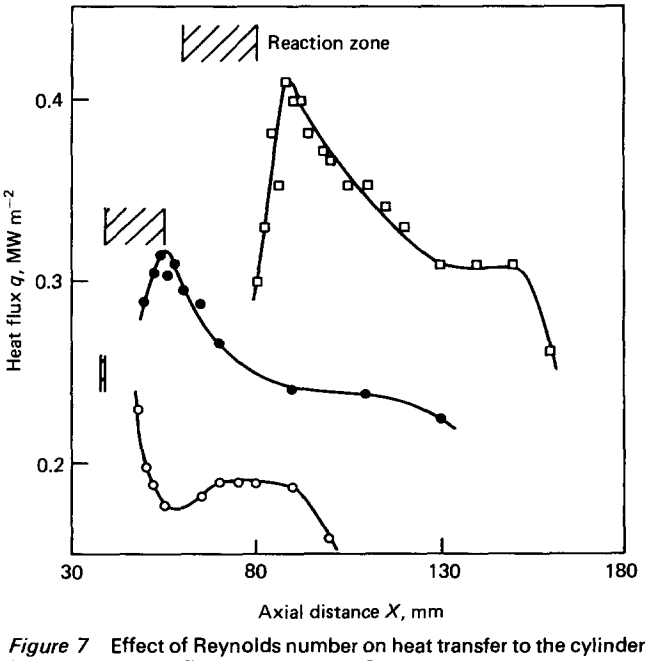

Figure 7 Effect of Reynolds number on heat transfer to the cylinder for stoichiometric flames. Key as Fig 2

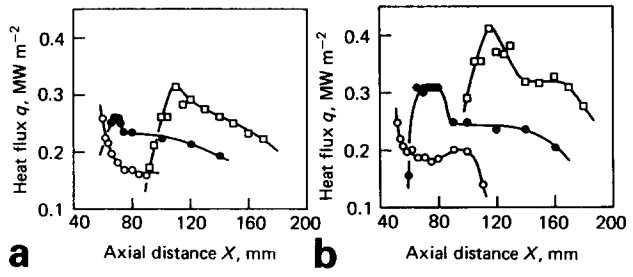

Figure 8 Effect of Reynolds number on heat transfer to the cylinder for (a) $\phi=0.8$ and (b) $\phi=1.2$ flames. Key as Fig 2

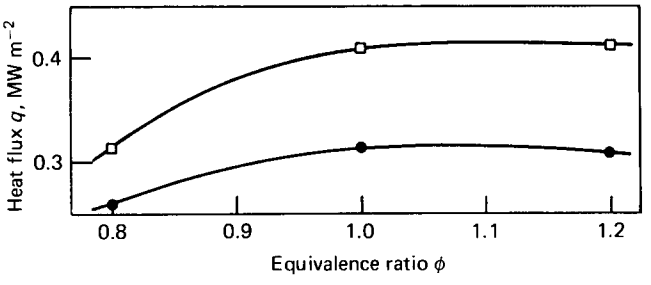

Figure 9 Variation of maximum rate of heat transfer to the cylinder with equivalence ratio. Key as Fig 2

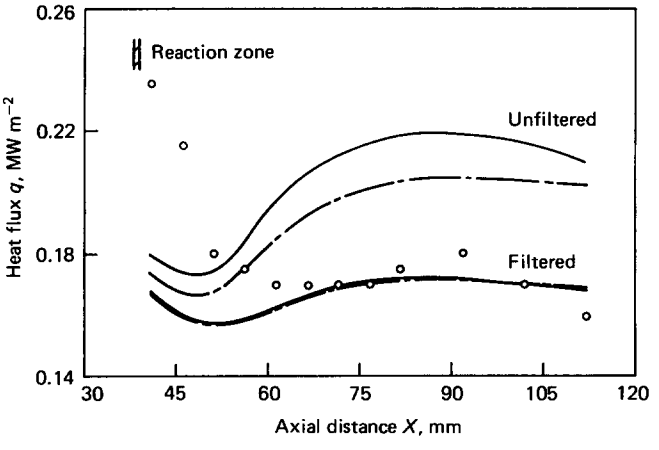

Figure 10 Comparison between theory and experiment for heat transfer to the body of revolution from the stoichiometric *Re=2000* flame (——— numerical solution, ——— empirical correlation).

predictions for heat transfer from the stoichiometric $Re=2000$ flame to the stagnation point of the body of revolution. Results labelled filtered and unfiltered in this figure were obtained using turbulence intensities derived with and without analogue filtering of measured instantaneous velocities, as described in the first part of the study.

Considering results based on filtered velocities, both prediction methods severely underestimate measured heat fluxes in the vicinity of the flame reaction zone. This is because of the abundance of nonequilibrium concentrations of reactive species in this region of the flame. Further downstream, where the flow approximates to chemical equilibrium conditions, reasonable agreement is obtained between predictions and experimental data. From approximately 100 mm, predictions begin to overestimate experimental data since they do not account for the unknown quantities of entrained air transferred to the flame centreline beyond this point. The shape of the predicted heat flux profiles through this flame is dictated by trends in the mean velocity and temperature of the flow as described in Ref 1. Free stream turbulence intensities also have an effect in causing maxima in the predictions at approximately 85 mm downstream, although no such trend is apparent in the experimental results.

The difference between predictions derived using filtered and unfiltered instantaneous velocities lies only in the turbulence intensity assigned to the free stream flow. The curves labelled unfiltered were determined using rms velocities, and hence turbulence intensities, of the free stream which contained effects arising from low frequency oscillations caused by large scale vortex rings present in the shear layer of the flames[1]. Predictions based on filtered velocities excluded the effect of these vortex rings. The difference between these two sets of predictions, and the extent to which results based on unfiltered turbulence intensities overestimate the experimental data, emphasises the need to exclude the effects of low frequency oscillations when determining turbulence intensities for use in heat flux predictions. Results obtained for the other flames considered in this study confirmed this finding.

In comparing theoretical results for heat transfer to both the hemispherical-nosed body and the circular cylinder with experimental data, comparisons were made only for those flames in which equilibrium regions were observed. Properties of the free stream required in deriving the predictions were defined at an axial location central to the flame equilibrium region, independently of the heat flux probe used to obtain experimental data. All the predictions given were obtained using filtered turbulence intensities.

Comparisons for the hemispherical-nosed probe are shown in Fig 11 in terms of the variation of heat flux in the flame equilibrium region with unburnt mixture equivalence ratio. Numerical solutions and predictions of the empirical correlation are seen to be in close agreement over the whole range of equivalence ratios examined. The predictions tend to underestimate experimental data over most of this range, although the maximum discrepancy between theory and experiment is 15%. Equivalent results for the cylindrical probe are given in Fig 12. Again, the empirical correlation is seen to agree reasonably well with experimental data, underpredicting the latter by a maximum of 14%. Numerical solutions, not shown in this figure, were always found to underestimate experimental results and by as much as 30%. Also, predictions for the cylindrical geometry were always less than equivalent results obtained for the hemispherical-nosed body by, on average, 16%. The latter finding is in broad agreement with predictions obtained by Galloway[8] for the case of heat transfer from turbulent air flows, where from a similar analysis to that used in the present work predictions for axisymmetric flows were found to be larger than equivalent two-dimensional results by approximately 11%. In the present analysis the disagreement between theory and experiment is most likely due to the constant K used in the eddy law, Eq (9), and to the simplicity of the eddy law itself.

With the exception of numerical solutions for the cylindrical geometry, predictions of the theoretical methods described are in reasonable agreement with experimental data. These

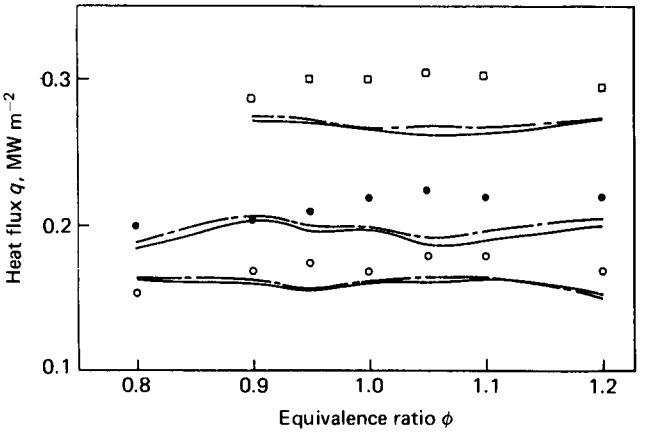

Figure 11 Effect of equivalence ratio on rate of heat transfer in the flame equilibrium region for the body of revolution. Key as Figs 2 and 10

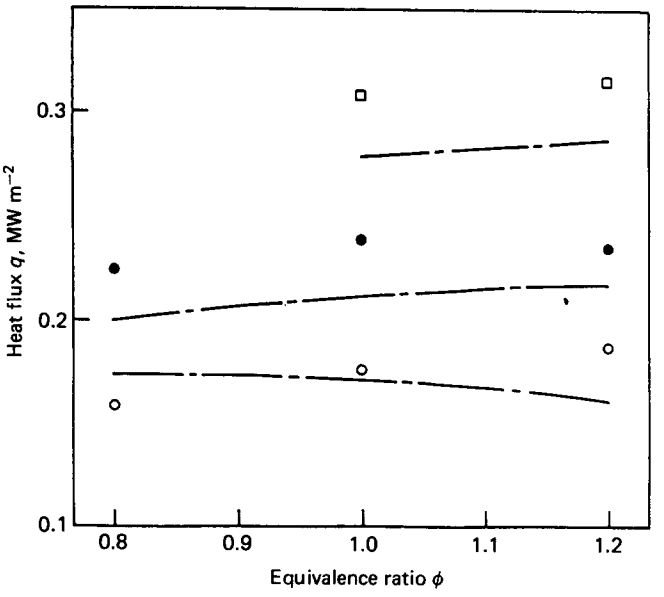

Figure 12 Effect of equivalence ratio on rate of heat transfer in the flame equilibrium region for the cylinder. Key as Figs 2 and 10

methods, and in particular the empirical correlations, can be used for the rapid computation of convective heat transfer rates from flames. Also, although validation has only been in terms of equilibrium flows, such conditions are encountered in a large number of industrial situations where heat transfer is due to forced convection of burnt gases.

Conclusions

A study of convective heat transfer from impinging flames has been completed by the presentation of heat transfer rates measured in premixed methane–air flames. Unburnt gas equivalence ratios from 0.8 to 1.2 have been examined, with burner exit Reynolds numbers ranging from 2000 to 12 000. Impingement heat transfer was determined at the stagnation point of a body of revolution and a circular cylinder.

Results obtained using both types of heat-receiving body demonstrate that the trends observed in measured heat flux profiles are mainly determined by variations in the mean velocity and temperature within a flame, with peak heat transfer rates occurring within or close to the flame reaction zone. Increases in Reynolds number lead to an increase in the peak heat flux attained within a flame and to a decrease in the axial extent of the flame equilibrium region. For a particular Reynolds number flow, variations in equivalence ratio away from approximately stoichiometric conditions lead to a shifting of the flame reaction zone, and hence the position of peak heat flux, downstream and to a decrease in the maximum rate of heat transfer from the flame. Heat transfer rates to the circular cylinder were found to be greater than those obtained using the body of revolution at all positions in a flame.

Predictions of stagnation point heat flux were made using numerical solutions of the appropriate boundary layer equations, and empirical correlations originally derived for nonreacting flow situations. Results obtained are in reasonable agreement with experimental data for flame equilibrium regions.

Acknowledgement

The authors would like to thank the British Gas Corporation for financing this project and for permission to publish.

References

1 Hargrave, G. K., Fairweather, M. and Kilham, J. K. Forced convective heat transfer from premixed flame—Part 1: flame structure. *Int. J. Heat and Fluid Flow*, 1987, **8**(1), 55–63

2 Hargrave, G., K. A study of forced convective heat transfer from turbulent flames. *Ph.D. Thesis*, Universiy of Leeds, 1984

3 Kilham, J. K. and Purvis, M. R. I. Heat transfer from hydrocarbon–oxygen flames. *Combustion and Flame*, 1971, **16**, 47–54

4 Dorrance, W. H. *Viscous hypersonic flow*. McGraw-Hill, 1962

5 Butler, J. N. and Brokaw, R. S. Thermal conductivity of gas mixtures in chemical equilibrium. *J. Chem. Phys.*, 1957, **26**, 1636–1643

6 Lees, L. Laminar heat transfer over blunt-nosed bodies at hypersonic speeds. *Jet Propulsion*, 1956, **26**, 259–269

7 Smith, M. C. and Kuethe, A. M. Effects of turbulence on laminar skin friction and heat transfer. *Phys. Fluids*, 1966, **9**, 2337–2344

8 Galloway, T. R. Enhancement of stagnation flow heat and mass transfer through interactions of free stream turbulence. *AIChE J.*, 1973, **19**, 608–617

9 Hargrave, G. K., Fairweather, M. and Kilham, J. K. Turbulence enhancement of stagnation point heat transfer on a body of revolution. *Int. J. Heat and Fluid Flow*, 1985, **6**, 91–98

10 Hargrave, G. K., Fairweather, M. and Kilham, J. K. Turbulence enhancement of stagnation point heat transfer on a circular cylinder. *Int. J. Heat and Fluid Flow*, 1986, **7**, 89–95

11 Numerical Algorithms Group, Nag Library Manual Mark 8, Volume 1, 1981

12 Fairweather, M., Kilham, J. K. and Nawaz, S. Stagnation point heat transfer from laminar, high temperature methane flames. *Int. J. Heat and Fluid Flow*, 1984, **5**, 21–27